Magnetic dimensionality crossover studies on the Heisenberg antiferromagnet $Rb_2FeCl_5 \cdot H_2O$

J. A. Puértolas and R. Navarro
Departamento de Física, Escuela Tecnica Superior de Ingenieros Industriales, Universidad de Zaragoza, Zaragoza, Spain

F. Palacio, J. Bartolomé, and D. González
Departamento de Física Fundamental, Facultad de Ciéncias, Universidad de Zaragoza, Zaragoza, Spain

Richard L. Carlin
Department of Chemistry, University of Illinois at Chicago, Chicago, Illinois 60680
(Received 23 January 1984; revised manuscript received 25 May 1984)

The heat capacity and the magnetic susceptibility between 1 and 33 K of antiferromagnetic $Rb_2FeCl_5 \cdot H_2O$ with spin $S=\frac{5}{2}$ are reported. Examination of the possible superexchange paths and analysis of the data allow us to conclude that the magnetic lattice presents low dimensionality at higher temperatures and then orders three dimensionally at 10.0±0.02 K. The experimental results have been fitted to a Heisenberg model with two effective intrachain and interchain exchange interactions. Theoretical values for the thermodynamic functions and characteristic fitting parameters J_z'/k_BT_c, $J_z'/k_BT(\chi_{max})$, and χ_{max} have been calculated by means of high-temperature-series analysis. The best fit gives $J_z'/k_B=-1.45\pm0.06$ K and $J_{xy}'/k_B=-0.15\pm0.07$ K. Spin-wave theory has been extended to this particular case of magnetic lattice crossover, the parameters resulting being in agreement with those from the paramagnetic region. A comparative analysis of the isostructural series $A_2FeCl_5 \cdot H_2O$ (A=K, NH_4, Rb) is carried out within the same theoretical framework.

I. INTRODUCTION

The series of compounds $A_2FeCl_5 \cdot H_2O$ (A=K, Rb, Cs, and NH_4) have received recent interest because of their special magnetic characteristics. The compounds order antiferromagnetically at temperatures below 20 K which permits the determination with reasonable accuracy of the magnetic contribution to the total heat capacity in each compound. Moreover, the presence of the Fe(III) ion in a high-spin, $S=\frac{5}{2}$, octahedral coordination makes these systems highly isotropic with respect to the magnetic properties and, therefore, they are good representatives of the Heisenberg model. Finally, an additional point of interest comes from the fact that the number of Fe(III) compounds studied showing magnetic ordering is rather small.

The thermomagnetic properties of $Cs_2FeCl_5 \cdot H_2O$ have already been reported.[1] The present contribution deals with the series of isomorphous compounds $A_2FeCl_5 \cdot H_2O$ where A=K, Rb, and NH_4. The main difference between this family of compounds and $Cs_2FeCl_5 \cdot H_2O$ is that the latter crystallizes in the *Cmcm* (D_{2h}^{17}) space group, while the rest of the compounds belong to the space group *Pmna* (D_{2h}^{7}).[2-5] Since differences in the magnetic behavior are expected, a separate study seemed appropriate.

Previous measurements of the heat capacity and the magnetic susceptibility for the K and NH_4 (Ref. 6) compounds and of the susceptibility for the Rb compound[2,7,8] were interpreted in terms of the presence of coupled antiferromagnetic linear chains. However, there are some features which point out that the problem remains unresolved. There are two sets of magnetic susceptibility measurements of the Rb compound available in the literature differing from each other in magnitude by about 8%; the model used to fit the experimental data for the three members of the series has only qualitative value and, finally, no comparative study of the magnetic properties of the series, showing the effects of the relatively small structural variations, has appeared so far.

The paper is set up as follows: First, heat capacity and magnetic susceptibility measurements for $Rb_2FeCl_5 \cdot H_2O$ are reported. Then the magnetic superexchange pathways are analyzed and the crossover theory for a Heisenberg antiferromagnetic linear chain ferromagnetically or antiferromagnetically coupled with neighboring chains is presented. In the absence of high-temperature-series (HTS) expansions for such a model with $S=\frac{5}{2}$, the $S=\infty$ case has been considered in the paramagnetic phase and a comparison with the experimental data is performed. In the next section predictions for the ordered phase, by means of the spin-wave theory for an $S=\frac{5}{2}$ Heisenberg system, are obtained and used to fit the experimental data with the same parameters as in the paramagnetic phase. Finally, the same theoretical model is used to reanalyze the heat capacity and magnetic susceptibility data available in the literature for the isomorphous K and NH_4 compounds. A good correlation between the crystalline structure and the magnetic properties is found.

II. EXPERIMENTAL

A. Heat capacity of $Rb_2FeCl_5 \cdot H_2O$

The heat capacity of $Rb_2FeCl_5 \cdot H_2O$ in the temperature range $1 < T < 35$ K has been measured in an adiabatic

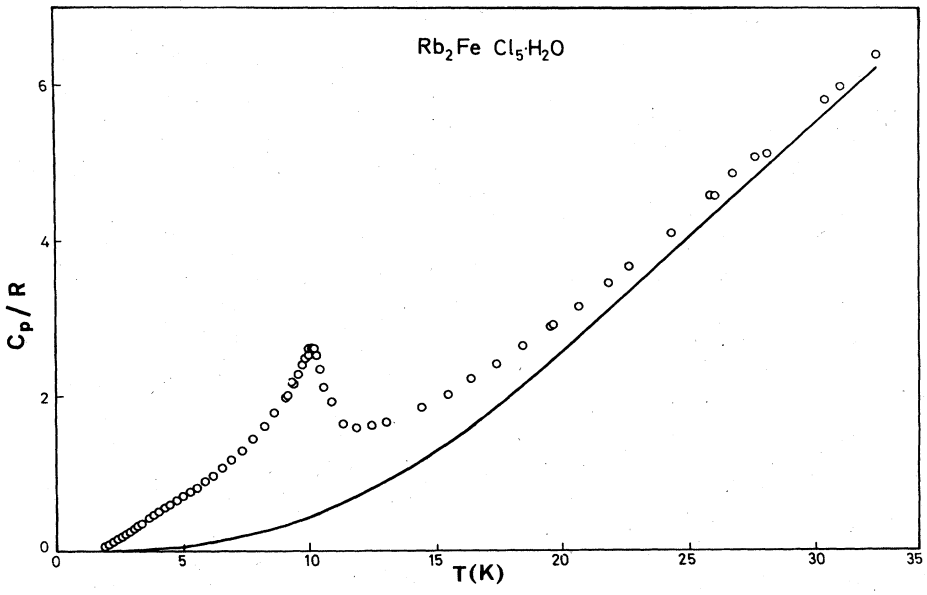

FIG. 1. Experimental heat-capacity data (open circles) and calculated lattice contribution (continuous line) for $Rb_2FeCl_5 \cdot H_2O$. In the evaluation of the lattice a value of $\mathscr{R}=0.1$ is used (see text).

calorimeter.[1,7] The sample was prepared by powdering crystals grown from an appropriate aqueous solution.[8] The results are shown in Fig. 1. A λ anomaly corresponding to the para-antiferromagnetic transition is found at $T_c=10.00\pm0.02$ K, in good agreement with $T_c=10.10\pm0.02$ K deduced from susceptibility data.[8] The shape of the high-temperature (HT) tail suggests the presence of low dimensionality of the magnetic properties.

B. Magnetic susceptibility of $Rb_2FeCl_5 \cdot H_2O$

Measurements of powdered- and single-crystal samples of $Rb_2FeCl_5 \cdot H_2O$ have been performed at zero field and selected temperature intervals with two different mutual inductance bridges. The frequency used was 332 Hz while the ac field amplitude never exceeded 0.5 Oe. The data show a rounded maximum at $T_{max}=12.5\pm0.3$ K and $\chi_{max}=0.088\pm0.01$ emu/mol. The easy axis for the antiferromagnetic alignment was found to be the a axis of the crystal, in agreement with previously reported measurements. An extrapolated value of $\chi_\perp(T=0\ \text{K})=0.089$ emu/mol was obtained.

These data are about 2% higher than those measured by O'Conner.[8] Since the experimental accuracy of this method is about 1%, the present data and that published in Ref. 8 are comparable. Thus, whenever a comparison is done below, only data of Ref. 8 will be considered.

III. SUPEREXCHANGE PATHWAYS

$Rb_2FeCl_5 \cdot H_2O$ crystallizes in the orthorhombic space group $Pnma$,[2] with four molecules per unit cell ($Z=4$), like the K and NH_4 isostructural compounds. The cell dimensions of the three systems are collected in Table I. The lattice is formed by discrete octahedral units, in which each iron atom is surrounded by five Cl atoms and the O from the water molecule. The octahedra are distorted tetragonally along the Fe—O bond, which is shorter than the equatorial Fe—Cl ones. The four complex ions, $[FeCl_5(H_2O)]^{2-}$, are arranged within the unit cell in two antiparallel pairs, the angle between the apical Fe—O directions of the octahedra and the a axis being 38°. In Fig. 2 a composition of four unit cells is represented,

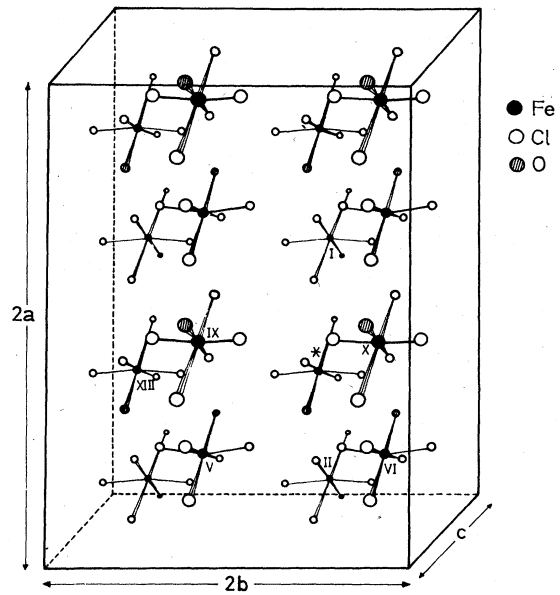

FIG. 2. Crystal structure of $Rb_2FeCl_5 \cdot H_2O$. The unit cell is doubled along the a and b axes. For clarity the Rb atoms are not included in the figure. The differences in size of the atoms indicate different a-b planes. *, Fe(*); I, Fe(1); II, Fe(2);. . .; XIII, Fe(13).

TABLE I. Elementary cell dimensions, in Å, of isostructural $A_2FeCl_5 \cdot H_2O$ (A = Rb, K, and NH_4) compounds.

	$A=NH_4$	$A=K$	$A=Rb$
a	13.706	13.75	13.825
b	9.924	9.92	9.918
c	7.024	6.93	7.100

where, for clarity, the Rb atoms have not been included.

Distances between a reference ion Fe(∗) and any of its 14 nearest Fe neighbors range from 6 to 9 Å. Several superexchange paths, all involving two atoms, can be identified. The first path, labeled by the associated exchange interaction J_1 (Fig. 3) would go through mixed oxygen-chlorine bridges forming zig-zag chains parallel to the b axis, connecting Fe(∗) to Fe(5) and Fe(6). On a comparative basis this interaction path can be considered to be the strongest, since it shows the minimum Cl-O distance, 3.18 Å. Moreover, hydrogen bonding involving the water molecule very likely contributes to the propagation of the interaction through this path.

A second and third interaction, denoted by J_2 and J_3 in Fig. 4, propagate in the a-c plane. Again double bridges Fe(∗)— Cl—O—Fe are formed for each interaction. Path J_2 connects Fe(∗) to Fe(1) and Fe(2) in a direction parallel to the a axis, and interaction path J_3 connects Fe(∗) to Fe(3) and Fe(4) in a direction parallel to the c axis. Each path has a weaker alternative for the same Fe(∗)—Fe connection through double bridges Fe(∗)—Cl—Cl—Fe.

A fourth interaction, J_4 in Fig. 3, propagates three dimensionally through the lattice. Again double bridges are formed, this time of the type Fe(∗)—Cl—Cl—Fe connections Fe(∗) to Fe(7), Fe(8), Fe(9), Fe(10), Fe(11), and Fe(12). In Fig. 3 the connection between Fe(∗) and Fe(12) is represented. Finally the interaction with atoms Fe(13) and Fe(14) may be considered almost negligible, since their separation from the Fe(∗) is 9 Å.

It has already been mentioned that J_1 seems clearly to be the strongest interaction path. It is not so clear, however, how to sort the J_2, J_3, and J_4 interactions by their relative strengths since the intensity of the exchange interactions is very sensitive to distance. Also, oxygen ligands provide exchange interactions stronger than chlorine ones, in part because of the lower electronegativity of the chlorine as compared with that of the oxygen. Therefore, the superexchange interaction path J_2 seems to be stronger than J_3 since the Cl-O distance in Fe—Cl—O—Fe bridges is shorter in J_2 (3.50 Å) than in J_3 (3.92 Å). However, that difference might be partially compensated by the shorter Cl-Cl distance in the Fe—Cl—Cl—Fe bridges along J_3 path (3.80 Å in J_3 versus 4.04 Å in J_2). On the other hand, J_4 seems to be the weakest interaction, since it propagates only through

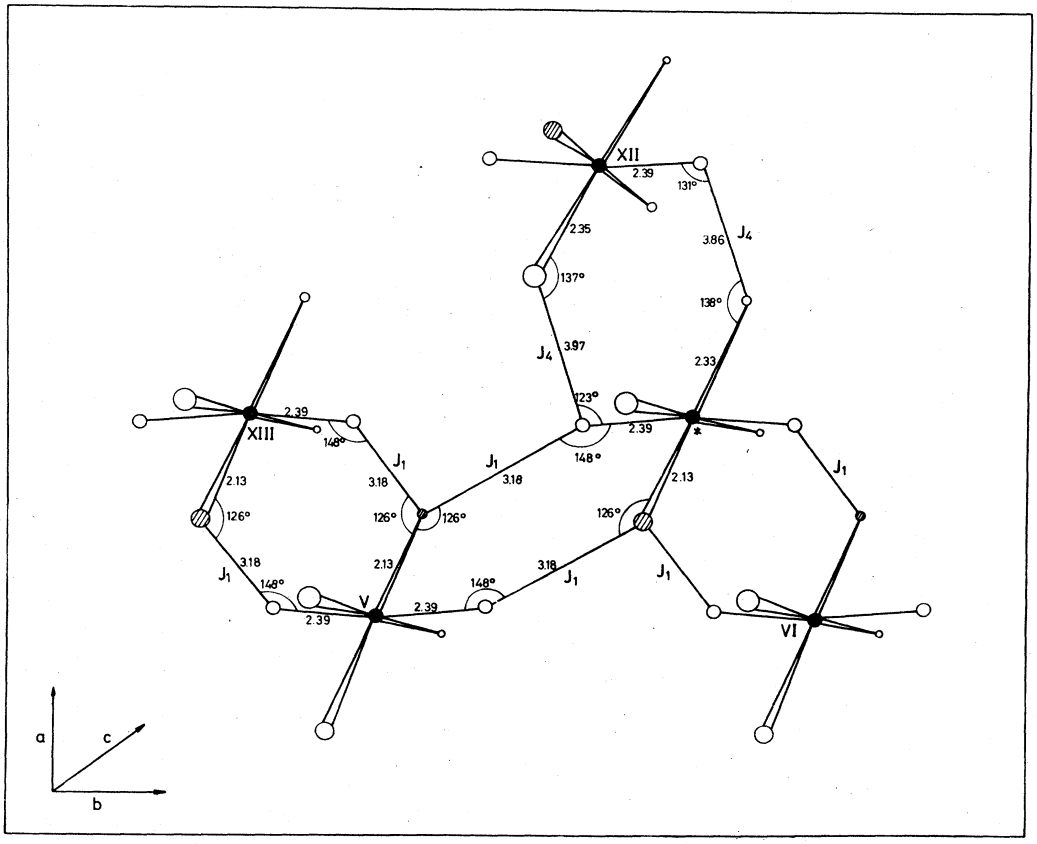

FIG. 3. Superexchange interaction paths J_1 and J_4 for $Rb_2FeCl_5 \cdot H_2O$. Only the relevant distances and angles have been indicated. Fe atoms are labeled as in Fig. 2.

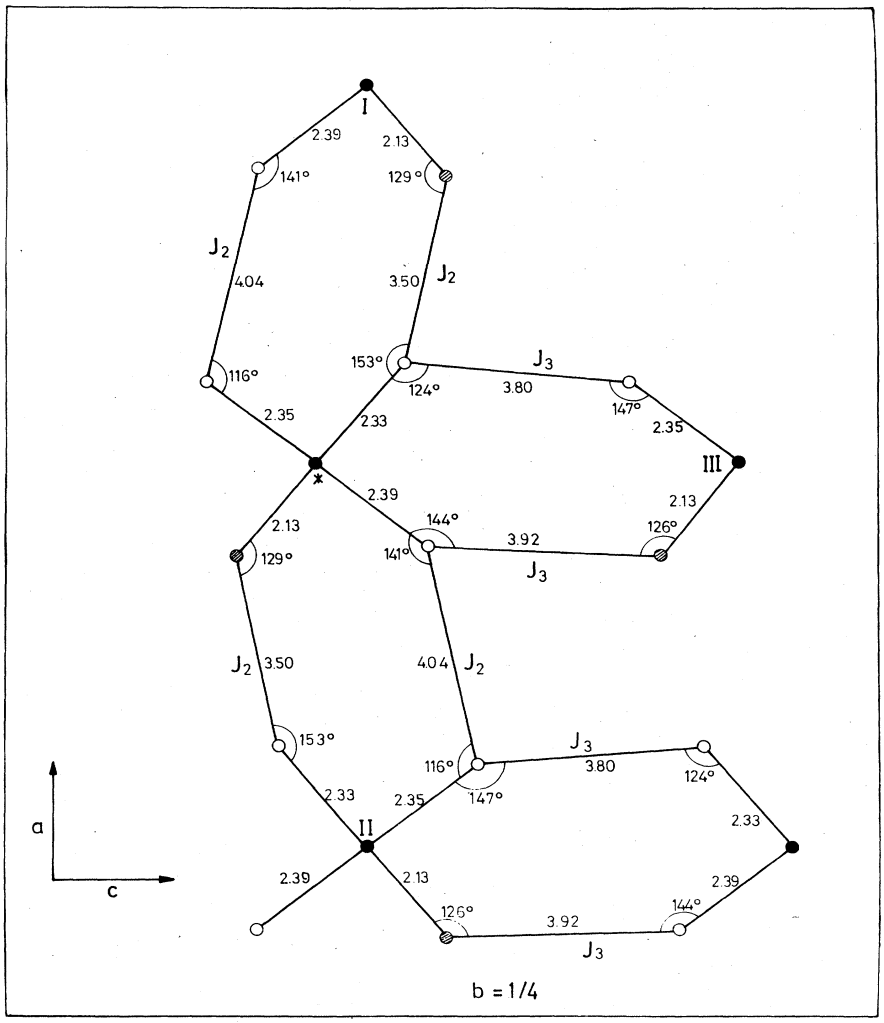

FIG. 4. Superexchange interaction paths J_2 and J_3 for $Rb_2FeCl_5 \cdot H_2O$ along plane $b = \frac{1}{4}$. Plane $b = \frac{3}{4}$ shows a correspondingly symmetric scheme. Fe atoms are labeled as in Fig. 2.

Fe—Cl—Cl—Fe bridges, with distances between the chlorine ligands of $d_{\text{Cl-Cl}} = 3.85$ and 3.97 Å. Moreover, the Fe—Cl bond distances are over 10% larger than the Fe—O one, supporting the assumption that $J_1 > (J_2 \geq J_3) > J_4$.

From the above analysis one can expect a certain low-dimensional magnetic behavior for $Rb_2FeCl_5 \cdot H_2O$ because of the larger strength of the J_1 superexchange interaction. However, pure linear chainlike properties cannot be expected since the J_2 and J_3 paths propagate non-negligible interactions to the four neighbors allocated in planes perpendicular to the J_1 path.

The (intrachain) interaction J_z will be identified with the J_1 one, and the (interchain) interaction J_{xy} will be identified with the average $J_{xy} = (J_2 + J_3)/2$. In this scheme, the interaction J_4 is neglected. Discrepancies of the data with the model will be a test of the adequacy of the simplifications chosen.

IV. STUDY OF THE DIMENSIONALITY CROSSOVER OF THE MAGNETIC LATTICE

The present problem belongs to the general case of a magnetic lattice which has predominantly low-dimensional interaction geometry with nearest-neighbor atoms along one direction and a weaker interaction with atoms placed in perpendicular planes. When the temperature is low enough for this secondary interaction to play a competing role, the magnetic properties of the system pass from low to higher dimensionality.

For all compounds of the $A_2FeCl_5 \cdot H_2O$ series the Fe(III) ions are surrounded by distorted octahedra and have a $^6S_{5/2}$ ground state. Spin-orbit coupling splits that state into three Kramers doublets with energy differences negligible in comparison with the temperatures at which the present measurements have been performed. In fact, since the anisotropy parameter has values $\alpha = 3.4 \times 10^{-3}$

for the Rb compound and $\alpha=8.5\times10^{-3}$ for the K one[9] the anisotropy field cannot produce significant splitting. The Lande g factor was measured with EPR spectroscopy of Fe(III) in the diamagnetic isostructural matrix $(NH)_4InCl_5\cdot H_2O$, obtaining a value of $g=2.014\pm0.003$.[10] Consequently, an isotropic Heisenberg model with $g=2$ and $S=\frac{5}{2}$ will be considered in what follows. The present work develops the theoretical framework for the $(d=1)$ to $(d=3)$ and $(d=2)$ to $(d=3)$ crossovers.

The only existing power-series expansions with inequivalent neighbors (i.e., linear chains coupled three dimensionally) for the Heisenberg model are for $S=\infty$. Only ten coefficients for the susceptibility and five for the heat capacity have been calculated so far.[11] Nevertheless, this result is useful in the present case as it is physically significant, above the critical temperature, to fit data for a $S=\frac{5}{2}$ system with the predictions for a $S=\infty$ one. This is so because the coefficients of χ and C_p as a function of the reduced temperature, $\tau=k_BT/JS(S+1)$, tend smoothly to the values for $S=\infty$ as S increases. In fact, for all magnetic lattices[12] which have been studied the values of the coefficients for $S=\frac{5}{2}$ are very close to those for $S=\infty$.

There are, nevertheless, qualitative differences between the classical Heisenberg (CH) model and the quantum one (finite S), even for the high-temperature-series results. One of the most relevant peculiarities of the CH model is that it gives the same position for the ferromagnetic (FM) and antiferromagnetic (AFM) reduced critical temperature, τ_c and τ_N, respectively, whereas for the $S=\frac{5}{2}$ Heisenberg Hamiltonian τ_c is smaller than τ_N (Ref. 13) [$\tau_N/\tau_c=1.012$ for the simple cubic (sc) lattice (Ref. 14)].

On the contrary, in the ordered region the $S=\infty$ model yields to conceptual difficulties; therefore, spin-wave theory for a Heisenberg Hamiltonian with $S=\frac{5}{2}$ and the experimentally observed anisotropy will be used in the ordered region.

A. Paramagnetic phase: Theoretical study

In this section, the characteristic parameters of the susceptibility and heat capacity as well as theoretical predictions for both χ and C_p as a function of the temperature are calculated. The calculations are based on the results of Lambeth and Stanley,[11] who use the Hamiltonian

$$H=-J_{xy}\sum_{\langle i,j\rangle_{(x,y)}}\vec{S}_i\cdot\vec{S}_j-J_z\sum_{\langle i,j\rangle_z}\vec{S}_i\cdot\vec{S}_j \tag{1}$$

where $\vec{S}_i$ is a classical vector in three dimensions, the first summation is over the nearest-neighbor pairs in the x-y plane, and the second summation runs over pairs along the chain direction (z direction). The series expansion can be developed as a double series of the parameter $K=J_>/k_BT$ and the ratio $\mathcal{R}=J_</J_>$, with $J_>=J_z$ and $J_<=J_{xy}$ in the linear-chain–sc crossover, and $J_>=J_{xy}$, $J_<=J_z$ in the square-planar-sc crossover.[15]

To start with, the position of the FM singularity, K_c has been analyzed, obtaining the roots of the Padé-approximant (PA) denominators[16] of the transformed susceptibility series $(\chi)^{1/\gamma}$ for different $\mathcal{R}$ values. The value $\gamma=1.405$ for the critical exponent[12,17] found for $J_z>0$ and $\mathcal{R}=1$ has been taken, and the universality hypothesis allows its use for any $\mathcal{R}\neq1$ (except for the limit $\mathcal{R}=0$ and ∞). Since the above value for γ is not the only one in the literature, e.g., $\gamma=1.375$ as deduced by Bowers *et al.*,[18] it is convenient to know the sensitivity of K_c to changes in γ. The calculations show that K_c changes about 2% when γ varies from 1.405 to 1.375, but this change in K_c is insignificant for the usual fitting purposes.

Once K_c is known, it is possible to calculate the theoretical prediction for $C_p(T)$ for every value of $\mathcal{R}$. Applying PA directly to the series expansions and taking into account the dispersion of the approximants, it is only possible to obtain reasonably accurate C_p estimations well away from the critical region. In order to have values of C_p as near as possible to the critical region, a somewhat different approach has been done. In the critical region one may assume a behavior for C_p, as K tends to K_c $(K<K_c)$, of the form[12]

$$C_p/R\sim A-B(1-\mathrm{K}/K_c)^{-\alpha} \tag{2}$$

where $\sim$ stands for "is asymptotically proportional to," and α is the critical exponent for the heat capacity. Then, following Domb and Bowers,[19] the ratio for each C_p/R series coefficient with the corresponding one from the expansion $(1-\mathrm{K}/K_c)^{-\alpha}$ has been calculated. If the series converges properly for sufficiently high order of the coefficients, these ratios should give the value of the critical amplitude B. Using $\alpha=-0.14$,[17] the sequence of ratios for $1>\mathcal{R}>0.3$, although increasingly scattered as $\mathcal{R}$ decreases, gives values of B reasonably consistent among each other for high orders of the coefficients, while for $\mathcal{R}<0.3$ the scatter in the coefficient ratios is so large that it renders impossible the determination of B. Once the parameters α, K_c, and B have been selected or estimated, the C_p curve can be extended down towards T_c applying PA to the expression

$$C_p/R=(PA)[(\mathrm{hts})+B(1-\mathrm{K}/K_c)^{-\alpha}]-B(1-\mathrm{K}/K_c)^{-\alpha}\,. \tag{3}$$

The PA's applied in order to obtain the C_p curves were the $[N/N-1]$, $[N/N-2]$, $[N-1/N]$, $[N-2/N]$, and so on. They are expressed in the usual nomenclature of $[N/D]$ for the PA of order N in the numerator and D in the denominator, with N and D compatible with the available number of terms in the series. The representative curves are shown in Fig. 5, where the error bars below $T=1.2T_c$ indicate the dispersion of the different PA at that temperature. Above $1.3T_c$ the dispersion becomes negligible.

The heat-capacity curves are independent of the signs of either J_z or $\mathcal{R}$, since in the high-temperature series of C_p, only the even powers of K and $\mathcal{R}$ are present for $S=\infty$. Then one cannot establish from C_p data alone whether J_z corresponds to a FM or AFM interaction, or determine the relative signs of J_z and J_{xy}. In order to decide on this point it is necessary to use the susceptibility series, since they contain both even and odd powers of K and $\mathcal{R}$.

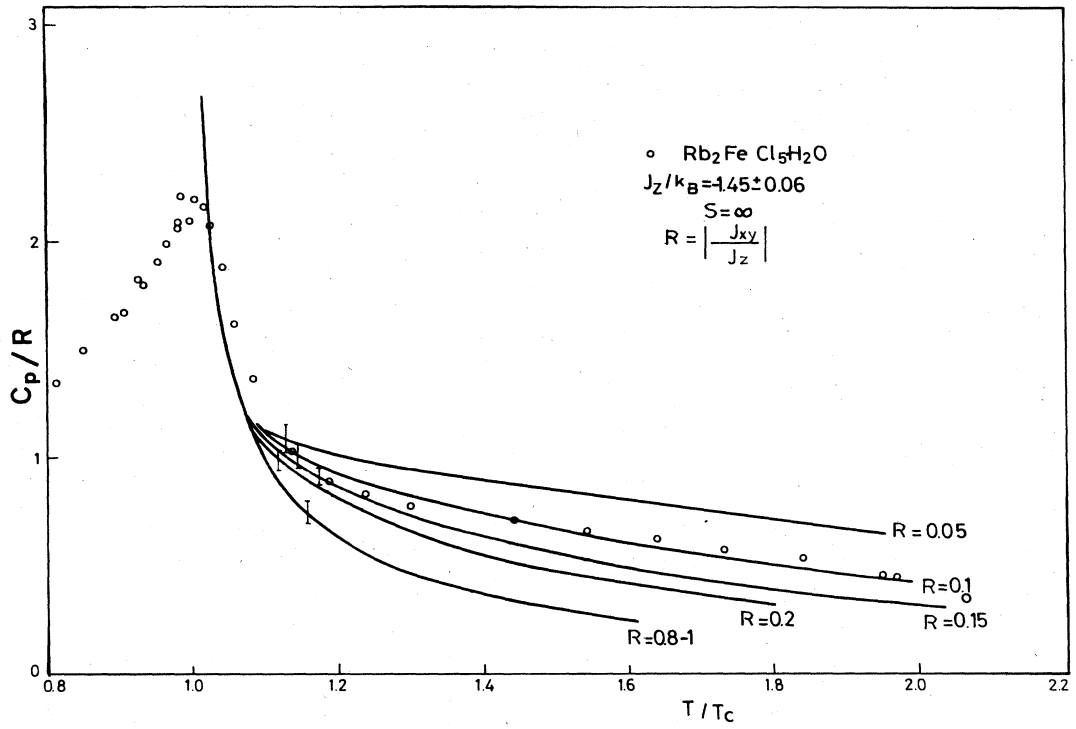

FIG. 5. Magnetic contribution to the heat capacity in the paramagnetic phase. Open circles: calculated from the measurements of $Rb_2FeCl_5 \cdot H_2O$ by subtracting the lattice contribution; continuous line: theoretical predictions for several values of the ratio J_{xy}/J_z.

In the analysis of the high-temperature zero-field susceptibility series, direct PA have been applied in order to increase the radius of convergence of the direct series.

Depending on the sign of both J_z and J_{xy}, there are eight alternatives. All these crossover possibilities are represented in Fig. 6 in a (J_z, J_{xy}) plane divided into octants. The present study is restricted to the nondivergent susceptibilities which correspond to octants 3 to 8.

Following a similar PA analysis method as applied for C_p, in each octant the susceptibility curves for fixed $\mathscr{R}$ and varying PA have been calculated as a function of K. The curves drawn in Fig. 7 are the best representatives,

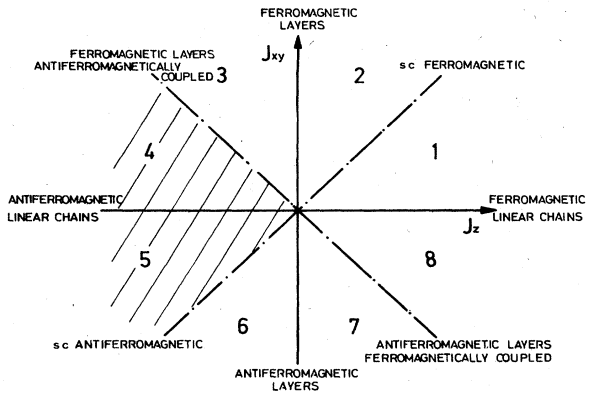

FIG. 6. J_z-J_{xy} graph showing the different alternatives for magnetic lattice crossover. These possibilities reduce to dashed octants 4 and 5, after the analysis of the magnetic heat capacity and $T(\chi_{max})$.

and the dispersion for the different PA curves is shown by the error bars, as above. As expected for AFM coupling, the curves show a rounded maximum, whose position and height, $K_{max}=J_>/k_BT(\chi_{max})$ and $\bar{\chi}_{max}=\chi_{max}J_>/N\mu_B^2g^2$, may now be determined, allowing a later fit with the experiments. From inspection of the curves for the linear chain to sc crossover shown in Fig. 7, one observes a reduction of height of the maximum and a decrease in its position in reduced temperature as the ratio $\mathscr{R}$ changes from the $1-d$ to the $3-d$ case.

Another way to determine the K_{max} position is by means of the analysis of the full susceptibility expression, whose maximum gives rise to a root in the PA denominator polynomial of the χ^{-1} series. The values obtained in this manner coincide with the previously deduced values, within the estimation error, thus validating both procedures.

Although some results for octants 3 to 8 are listed in Ref. 15 for certain values of $\mathscr{R}$, new results for octants 4, 5, and 8 are listed in Table II, with relevant values of $\mathscr{R}$ for our fitting purposes.

In order to compare the theoretical susceptibility $\bar{\chi}$ for $S=\infty$, with the experimental $(S=\frac{5}{2})$ it is necessary to scale them using the relation

$$\bar{\chi}=3\chi_{exp}J'_>/N\mu_B^2g^2S(S+1)\,, \tag{4}$$

$$J_>=2J'_>S(S+1)/3\,, \tag{5}$$

where $J'_>$ refers to the $S=\frac{5}{2}$ system.

B. Paramagnetic phase: Analysis of the $Rb_2FeCl_5 \cdot H_2O$ data.

The interpretation of the $\chi(T)$ and $C_p(T)$ data of the Rb compound can be simplified by taking into account

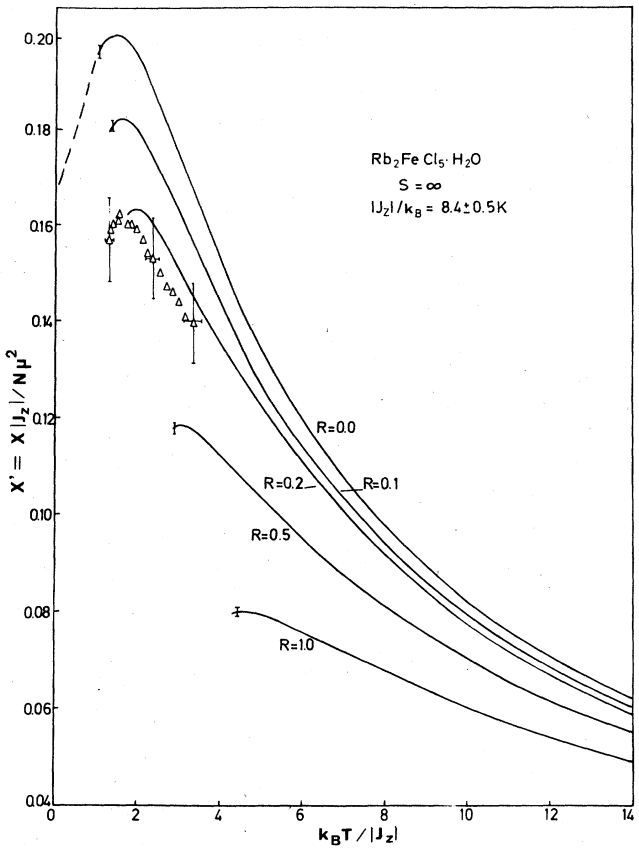

FIG. 7. Theoretical predictions for the susceptibility in the paramagnetic phase (continuous lines), for several values of the ratio J_{xy}/J_z, compared with data from $Rb_2FeCl_5 \cdot H_2O$ (open triangle).

that $\chi(T)$ shows no singularity and that the J_z exchange predominates over J_{xy}, as discussed in Sec. II. The first condition excludes all cases belonging to octants 1 and 2 while the second one eliminates those covered by the octants 3, 6, and 7.

Then, the magnetic behavior of $Rb_2FeCl_5 \cdot H_2O$ should fit in one of the octants 4, 5, or 8; that is, it should correspond to AFM chains, either ferromagnetically (octant 4) or antiferromagnetically ordered (octant 5), or FM chains antiferromagnetically ordered (octant 8).

One expects that the $C_p(T)$ and $\chi(T)$ experimental data may be fitted unambiguously with just one set of J_z and $\mathscr{R}$ parameters. To obtain the fit, a first scan is done substituting the three values $T_c = (10.01 \pm 0.02)$ K,

$$T(\chi_{\max}) = (12.5 \pm 0.3)\ K,$$

and $\chi_{\max} = (0.088 \pm 0.001)$ emu/mol in Table II, for varying $\mathscr{R}$ values. The discrepancies of the J_z values within the set deduced for any $\mathscr{R}$ value belonging to octants 8 and 4 are so large that they exclude those cases.

On the other hand, a reasonable consistency (dispersion of about 10% in J_z) is obtained for $\mathscr{R} = 0.1$, i.e., in octant 5, with the average value $J_z/k_B = -8.4 \pm 0.5$ K (CH model $S = \infty$). One concludes that the system is formed from antiferromagnetic linear chains, coupled antiferromagnetically.

The above values may be tested by substituting them into the $\chi(T)$ theoretical prediction and comparing the result to the experimental data in the whole temperature range. This is depicted in Fig. 7, where one observes that the experimental susceptibility follows the prediction for $\mathscr{R} = 0.1$ with a maximum discrepancy of 10%.

The magnetic heat capacity C_m is also very sensitive to the lattice dimensionality and therefore it can be used for an independent determination of $\mathscr{R}$. In fact, plotting the experimental C_m/R versus T/T_c, the shape becomes dependent only on $|\mathscr{R}|$, allowing its determination by comparison to theory, in principle. However, the lack of a proper estimation of the lattice contribution for this case precludes the determination of C_m. Notwithstanding, the C_p data may be useful to check pairs of J_z and $\mathscr{R}$ values in the following way. The theoretical C_m curve for the given crossover may be subtracted from the HT experimental C_p data. The temperature range used in this operation is limited to that in which the PA's of the HTS for C_m has a dispersion smaller than 5%. The lattice heat capacity obtained, C_1, in this restricted region has been fitted by least-square methods to an odd power polynomial like $AT^3 + BT^5 + CT^7$ (Ref. 20) and is then extrapolated down to 0 K. The difference between the experimental C_p and the estimated C_1 is, consequently, the magnetic contribution to the heat capacity in the whole temperature range.

The anomalous entropy content obtained from C_m is close to the theoretical one $\Delta S_m = R \ln(2S+1) = 1.79$ only for values of $\mathscr{R}$ between $\mathscr{R} = 0.1$ ($\Delta S_m = 1.88$ R), and $\mathscr{R} = 0.2$ ($\Delta S_m = 1.72$ R). Any other $\mathscr{R}$ value yields an anomalous entropy content differing more than 10% from the theoretical value. A lattice contribution calculated for $\mathscr{R} = 0.1$ is depicted in Fig. 1.

From the analysis of the heat capacity and magnetic

TABLE II. Representative values of $|J_z|/k_BT_c$, $|J_z|/k_BT(\chi_{\max})$, and $\bar{\chi}_{\max} = \chi_{\max}|J_z|/N\mu_B^2 g^2$ for octants 4, 5, and 8 of Fig. 9.

	$\lvert\mathscr{R}\rvert$	1	0.5	0.3	0.1	0.05
	$\lvert J_z\rvert/k_BT_c$	0.3213	0.358	0.479	0.840	1.17
$J_z<0,\ \mathscr{R}>0$	$\lvert J_z\rvert/k_BT(\chi_{\max})$	0.217	0.334	0.437	0.616	0.97
	$\bar{\chi}_{\max}$	0.0796	0.1183	0.145	0.182	0.192
$J_z<0,\ \mathscr{R}<0$	$\lvert J_z\rvert/k_BT(\chi_{\max})$	0.235	0.350	0.45	0.627	0.67
	$\bar{\chi}_{\max}$	0.239	0.231	0.224	0.214	0.207
$J_z>0,\ \mathscr{R}<0$	$\lvert J_z\rvert/k_BT(\chi_{\max})$	0.227	0.34	0.50	0.84	1.2
	$\bar{\chi}_{\max}$	0.119	0.240	0.397	1.24	2.5

susceptibility in the paramagnetic region the value $J_z/k_B=-8.4\pm0.5$ K (CH) is obtained. This value slightly differs from the $J_z/k_B=-7.7\pm0.4$ K given in a preliminary report[15] although it overlaps with it. The distinct procedure followed here in the evaluation of the data accounts for the difference. The above J_z/k_B corresponds in a $S=5/2$ system to $J_z'/k_B=-1.45\pm0.06$ K. Also from the value of $\mathcal{R}$ one obtains $J_{xy}'/k_B=-0.14\pm0.04$ K; that is, an order of magnitude lower, in agreement with the expected relative intensities in the pathways discussed in Sec. II.

C. Ordered phase: Spin-wave theory

In order to extend the study of the magnetic dimensionality crossover to the ordered region, the suitable spin-wave theory of AFM chains along the "z" direction coupled antiferromagnetically in the "x-y" plane should be developed. Let us choose a Heisenberg Hamiltonian with small anisotropy, such as

$$\mathcal{H}=2J_z'\sum_{\langle i,j\rangle_z}\vec{S}_i\cdot\vec{S}_j+2J_{xy}'\sum_{\langle i,j\rangle_{(x,y)}}\vec{S}_i\cdot\vec{S}_j-g\mu_B H_A\left[\sum_{i=1}^{a}S_i^z+\sum_{j=1}^{b}S_j^z\right], \quad (6)$$

where J_z' and J_{xy}' denote the intrachain and interchain interactions, respectively. H_A is the anisotropy field, the superscripts "a" and "b" label the two magnetic sublattices, and S is equal to $\frac{5}{2}$.

Using the Holstein-Primakoff relations to map the spin deviations to the bosonic space (free magnons) and applying the usual Fourier transformation to the reciprocal space,[21] the Hamiltonian (6) may be expressed as a function of creation and annihilation operators for both sublattices

$$\begin{aligned}\mathcal{H}=&E_0+2J_{xy}'Sq^{(x,y)}\Sigma_{\vec{k}}\gamma_{\vec{k}}^{(x,y)}(a_{\vec{k}}b_{\vec{k}}+a_{\vec{k}}^{\dagger}b_{\vec{k}}^{\dagger})\\&+2J_z'Sq^{(z)}\Sigma_{\vec{k}}\gamma_{\vec{k}}^{(z)}(a_{\vec{k}}b_{\vec{k}}+a_{\vec{k}}^{\dagger}b_{\vec{k}}^{\dagger})\\&+(2J_{xy}'Sq^{(x,y)}+2J_z'Sq^{(z)}\\&+g\mu_B H_A)\Sigma_{\vec{k}}(a_{\vec{k}}^{\dagger}a_{\vec{k}}+b_{\vec{k}}^{\dagger}b_{\vec{k}}) \quad (7)\end{aligned}$$

with

$$E_0=-NS^2(q^{(x,y)}J_{xy}'+q^{(z)}J_z')-g\mu_B H_A SN\ ,$$

where higher-order terms have been neglected, $q^{(z)}$ and $q^{(x,y)}$ are the number of nearest neighbors in the z direction and in the x-y plane, respectively, the γ functions being

$$\gamma_{\vec{k}}=\frac{1}{q^{(z),(x,y)}}\sum_{(\mathrm{NN})(z),(x,y)}\exp i(\vec{k}\cdot\vec{r}^{(z),(x,y)})$$

with summations extended only to nearest neighbors.

If one defines the parameter $\xi=q^{(x,y)}J_{xy}/q^{(z)}J_z$, and the anisotropy parameter $\alpha=H_A/H_E$, then $H_E=2q^{(z)}J_z(1+\xi)S/g\mu_B$ and the effective number of nearest neighbors becomes ξ dependent, $q=q^{(z)}(1+\xi)$. Consequently the effective γ function takes the form

$$\gamma_{\vec{k}}^{(z)}=(\gamma_{\vec{k}}^{(z)}+q\gamma_{\vec{k}}^{(x,y)})/(1+\xi)\ ,$$

and the Hamiltonian Eq. (6) is transformed to another with the same form as if it were for equivalent neighbors

$$\begin{aligned}\mathcal{H}=&E_0+2J_z'Sq\Sigma_{\vec{k}}\gamma_{\vec{k}}(a_{\vec{k}}b_{\vec{k}}+a_{\vec{k}}^{\dagger}b_{\vec{k}}^{\dagger})\\&+2J_z'Sq(1+\alpha)\Sigma_{\vec{k}}\gamma_{\vec{k}}(a_{\vec{k}}^{\dagger}a_{\vec{k}}+b_{\vec{k}}^{\dagger}b_{\vec{k}})\ . \quad (8)\end{aligned}$$

This formal equivalence allows us the use of standard spin-wave theory,[21] adapting it for every crossover case. Thus, for the case of AFM linear chains AFM coupled with four neighbors the effective γ function is

$$\gamma_{\vec{k}}=1/(1+\zeta)[\cos k_z a_z+\zeta/2(\cos k_x a_x+\cos k_y a_y)]$$

with

$$\zeta=2J_{xy}'/J_z'=2\mathcal{R}\ .$$

In Figs. 8–10 we have represented the heat capacity and the parallel and perpendicular susceptibility

$$\bar{\chi}_{\parallel}=\chi_{\parallel}J_z'/Ng^2\mu_B^2\ ,\ \bar{\chi}_{\perp}=\chi_{\perp}J_z'/Ng^2\mu_B^2$$

of $Rb_2FeCl_5\cdot H_2O$ for several values of $\mathcal{R}$ and the anisotropy parameter $\alpha=3.4\times10^{-3}$, determined experimentally.[9] The curves are valid up to $\tau<\tau_c/2$, since free spin-wave theory loses its applicability above that temperature.

D. Ordered phase: Analysis of the $Rb_2FeCl_5\cdot H_2O$ data

With the spin-wave theory developed above it is now possible to check whether the set of parameters J_z' and $\mathcal{R}$ obtained in the paramagnetic region is compatible with the low-temperature experimental results. In contrast to the paramagnetic region, the absence of characteristic points and the interdependency of J_z'/k_B and $\mathcal{R}$ in the range $\tau<\tau_c/2$ precludes the determination of an independent set of parameters. However, a check can be done by fixing $J_z'/k_B=-1.45$ K and comparing the theoretical C_m curves, now only a function of $\mathcal{R}$ and τ_c, with the data. In Fig. 8 the experimental C_m deduced by subtraction of the estimated C_1, as a function of k_BT/J_z' together with the theoretical predictions for a set of $\mathcal{R}$ values is represented. From the figure it is clear that values between $\mathcal{R}=0.1$ and 0.15 are the most appropriate to fit the data, in accordance with the results of $\mathcal{R}$ obtained for C_p in the paramagnetic phase.

As a further check, considering the J_z' constant fixed above, the experimental $\chi_{\parallel}$ (a crystallographic axis) and $\chi_{\perp}$ (b axis) data has been compared with the corresponding theoretical prediction for different $\mathcal{R}$. The best fit for $\chi_{\parallel}$ and $\chi_{\perp}$ lies about $\mathcal{R}=0.15$ (see Figs. 9 and 10) in full agreement with the C_m fit in the ordered phase and similar to the results obtained in the paramagnetic region. This accordance validates the procedures applied in Secs. IV B and IV D, and, what is more important, proves that the present system follows the model of AFM chains, AFM coupled with four neighboring ones, unambiguously.

E. Analysis of the $K_2FeCl_5\cdot H_2O$ data

It is now possible to reanalyze the data for the isomorphous K and NH_4 compounds within the same theoretical

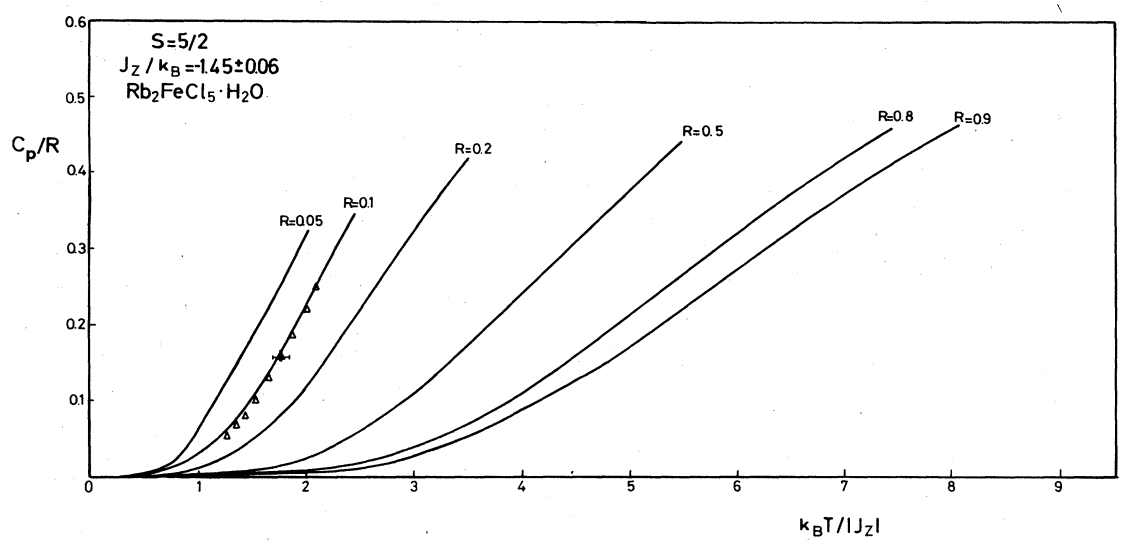

FIG. 8. Theoretical predictions for the heat capacity in the antiferromagnetic phase (continuous lines), for several values of the ratio J_{xy}/J_z, compared with data from $Rb_2FeCl_5\cdot H_2O$ (open triangle).

scheme and with the same procedure as with the Rb salt.

The relative differences in the cell dimensions, listed in Table I, affect the distances and angles in the interaction paths modifying the relative strengths of the exchange paths discussed for the Rb compound. Therefore, the microscopic changes can be correlated qualitatively with their effects in the thermodynamic (χ and C_p) behavior. In $K_2FeCl_5\cdot H_2O$ the unit-cell parameter c is 2.4% smaller than in the Rb analog. Assuming a dependency of superexchange paths with distance of the type r^{-11}, as is the case for singly-bridged paths, an increase of at least 30% in the value of J_3 could be estimated. However, the strength of the superexchange paths J_1 and J_2 should remain almost constant because the distances and angles suffer smaller changes.

The above comparative analysis yields a magnetic dimensionality crossover similar to the Rb one but with a stronger coupling between neighboring chains. The comparison of the theoretical results for the paramagnetic phase with the characteristic experimental values $T_c=14.06\pm0.01$ K, $T(\chi_{max})=16.0\pm1.5$ K, and $\chi_{max}=0.068\pm0.001$ emu/mol (Ref. 6) give a best value of $J_z=-8.4\pm0.5$ K for $\mathcal{R}=0.20-0.35$. A difference of about 10% in the maximum height of the susceptibility should be noted.

In order to analyze the heat capacity data of the K compound, the same indirect procedure as for the Rb case has been used. First the calculated HT magnetic tail for a given value of $\mathcal{R}$ is subtracted, and the difference, i.e., C_1, is fitted with a polynomial. The anomalous magnetic entropy is then estimated from the difference of the experimental data and the polynomial, both extrapolated to 0 K. For the values of $\mathcal{R}=0.2$ and 0.3, the magnetic entropy values $\Delta S_m/R=1.87$ and 1.91 are obtained, which are a few percent higher than the theoretical ones. Because of the errors involved in the procedure any value in the range $0.3>\mathcal{R}>0.1$ is equally valid.

On the other hand, the analysis of the C_p data in the

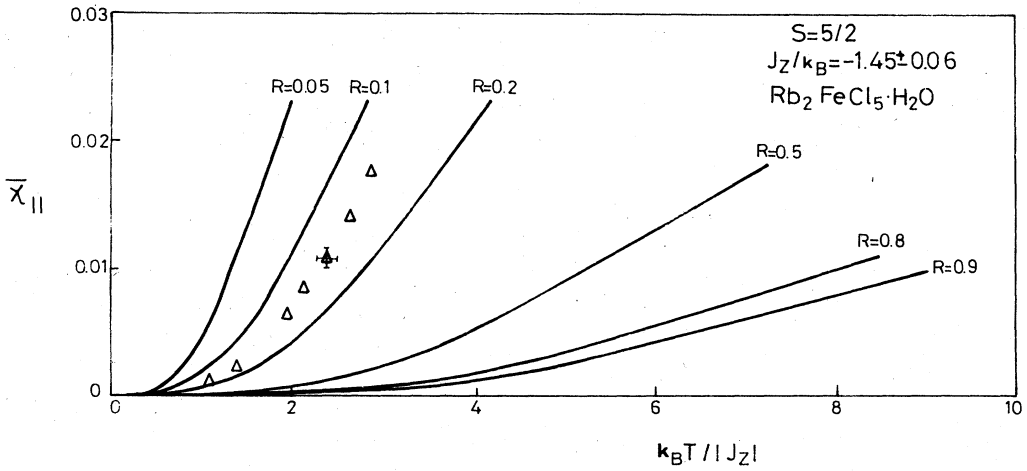

FIG. 9. Theoretical predictions for the $\chi_{||}(T)$ in the antiferromagnetic phase (continuous lines), for several values of the ratio J_{xy}/J_z, compared with data from $Rb_2FeCl_5\cdot H_2O$ (open triangle).

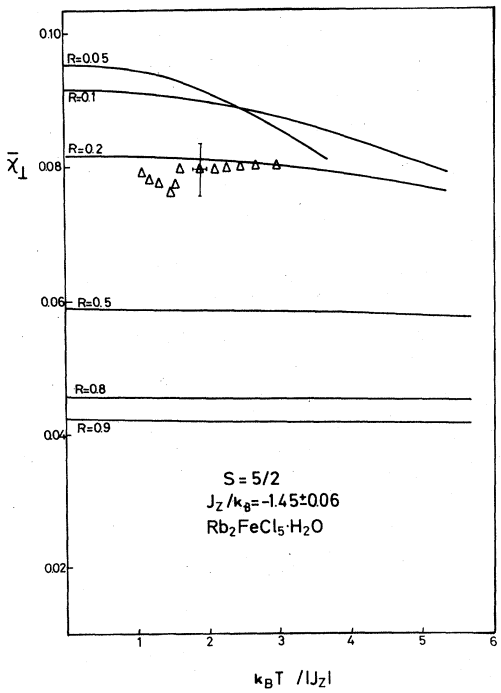

FIG. 10. Theoretical predictions for the $\chi_\perp(T)$ in the antiferromagnetic phase (continuous lines), for several values of the ratio J_{xy}/J_z, compared with data from $Rb_2FeCl_5 \cdot H_2O$ (open triangle).

spin-wave region cannot give a better determination for $\mathscr{R}$, because the available data are still above the temperature range in which the spin-wave prediction holds. The $\chi_{||}$ and $\chi_\perp$ data at low temperature may be fitted with the above $\mathscr{R}$ and J_z parameters properly scaled, but the discrepancy in the height of χ, present already in the Rb case, still remains.

F. Analysis of $(NH_4)_2FeCl_5 \cdot H_2O$ data

The compound $(NH_4)_2FeCl_5 \cdot H_2O$ shows differences with respect to the Rb analog, in the unit-cell size, a and c being smaller in the former by about 0.9% and 1.0%, respectively. Such changes should increase the strength of J_1 (see part III) and therefore should enhance the one-dimensional character in the magnetic properties.

The published data[6] of the heat capacity shows two anomalies at $T_c = 7.25 \pm 0.01$ K and $T_c' = 6.87 \pm 0.01$ K while in the susceptibility the double anomaly is not appreciable. Besides, the measurements do not present an AFM parallel easy axis. These problems make uncertain the interpretation of the data. However, the tentative assumption that the paramagnetic AFM ordering takes place at the higher critical temperature, and that T_c' is due to a spin realignment allows us to test the crossover theory.

The insertion of the experimental values $T_c = 7.25 \pm 0.01$ K, $T(\chi_{max}) = 11.7 \pm 0.1$ K and $\chi_{max} = 0.083 \pm 0.001$ emu/mol to the predictions of Table II gives the best value for the set, $J_z/k_B = -9.0 \pm 0.9$ K in the range $0.03 < \mathscr{R} < 0.05$. Since $\mathscr{R}$ is so low, this system appears to have the lowest lattice dimensionality character of the series. Indeed, the analysis of the heat capacity HT magnetic tail, in terms of the crossover theory, indicates that $\mathscr{R} < 0.08$ for the most unfavorable subtraction of the lattice heat capacity. All these facts agree with the expected enhancement of the low dimensionality, discussed on the basis of the larger contraction along the c axis. However, the discrepancy between the theoretical prediction for $\chi(T)$ with the above J_z and $\mathscr{R}$ yielding values 15% higher than the experimental ones as in the Rb and K cases, is again present.

In the ordered region only the perpendicular susceptibility is considered in view of the difficulties mentioned above. The best fit is obtained for $J_z'/k_B = -1.5 \pm 0.1$ K and $\mathscr{R} = -0.15 \pm 0.05$, i.e., a higher ratio than that obtained in the paramagnetic range. On the other hand, if one substitutes in the theory the values of $J_z'/k_B = -1.50$ K and $\mathscr{R} = -0.05$ from the HT fit, the prediction becomes 15% higher than the experiment. This discrepancy is similar to the rest of the susceptibility fits.

V. DISCUSSION

From the analysis of the available data for the series in terms of the crossover theory developed here, a collection of the exchange-interaction constants J_z' and J_{xy}' is obtained. They are listed in Table III, where for comparison, the results obtained by McElearney[6] and O'Connor[8] are included. Although reasonably similar values of J_z' have been derived, the difference in J_{xy}' is very pronounced.

The reason for the difference lies in the approximation made by these authors in their fit of the data. They consider the $S = \infty$ prediction for linear chains and couple them with an interchain molecular field (MF). This ap-

TABLE III. Exchange constants as calculated from the fit in both the paramagnetic (PM) and ordered (SW) phases for the three compounds of the series. For comparative purposes results from the molecular field (MF) approach of McElearney (Ref. 6) and O'Connor (Ref. 8) are also included.

			$Rb_2FeCl_5 \cdot H_2O$	$K_2FeCl_5 \cdot H_2O$	$(NH_4)_2FeCl_5 \cdot H_2O$
From crossover theory	PM phase	J_z'/k_B	-1.45 ± 0.06 K	-1.44 ± 0.05 K	-1.5 ± 0.1 K
		J_{xy}'/k_B	-0.15 ± 0.07 K	-0.4 ± 0.1 K	-0.06 ± 0.02 K
	SW phase	J_z'/k_B	-1.45 K (fixed)		
		J_{xy}'/k_B	-0.15 ± 0.08 K		
MF Theory		J_z'/k_B	-1.39 K	-1.55 K	-1.24 K
		J_{xy}'/k_B	-0.47 K	-0.76 K	-0.72 K

proach has been useful for systems with $|J'_{xy}| \ll |J'_z|$ in the description of the linear-chain susceptibility.

The position of the maximum is then related practically to J'_z, while its height is determined by J'_{xy}. As a consequence, in the fit of the experimental data with the MF model all errors and departures from the model are driven to the value of the parameter J'_{xy}. This results in values of J'_{xy} which are much higher than those obtained with a complete crossover theory. Other problems in the comparison are the inconsistencies in the susceptibility data found in the literature already mentioned in the experimental section, which affect the height of $\chi_{\max}$ and correspondingly the deduced J'_{xy} value.

The inadequacy of the linear-chain model corrected by a MF is even more apparent in the magnetic heat capacity, as the λ anomalies are similar in height to those found in three-dimensional systems[22] and consequently that approach is not applicable, even though the $\chi(T)$ data could be fitted.

The present model overcomes this incompatibility as it is capable of dealing quantitatively with C_m and χ data simultaneously, correlating microscopic and macroscopic properties for all members of the series.

The trend of increasing intrachain interaction for decreasing value of the a edge of the unit cell is clearly obtained. The interchain interaction follows the trend $K > Rb > NH_4$ which is explained in terms of the relative values of the exchange interactions $J_1 > J_2 = J_3$.

The model allows a reasonable fit of the heat capacity and susceptibility data although minor discrepancies remain. In the K and NH_4 compounds a systematic discrepancy between the experimental χ values and the calculated ones with the deduced exchange constant is detected.

It is convenient to analyze the alternative which could lower these χ values, improving the fit. First, $J_2 \neq J_3$ may be considered, but this lowers the magnetic dimensionality and then the calculated χ values are expected to be higher. On the contrary, if J_4 is considered, as a non-negligible superexchange interaction, the three-dimensional character in the magnetic model increases and hence, the expected values for the susceptibility would decrease. In the analysis of the superexchange paths the interaction path labeled as J_4 was considered as negligible, because the Fe-Cl-O-Fe bridges of the pathways J_2 and J_3 were assumed to be stronger than the Fe-Cl-Cl-Fe bridges of the J_4 path. However, it seems reasonable that, although weak, the large number of J_4 pathways (six) could, together, give a non-negligible contribution. Unfortunately, there is not a suitable model available with so many inequivalent exchange constants.

A tentative estimation of a nonzero J_4 exchange constant was done, by means of a model considering nearest and next-nearest neighbors.[23] Though a fit was possible, the J_4 value was inconsistent with the data and the expected relative values of the exchange constants. It may be concluded that the thermodynamic data analyzed here are not adequate to determine so many parameters.

Finally, it should be noted that this is the first time that crossover theory for the Heisenberg model has been applied. Previous work on the crossover study referred to the Ising system.[24] In this case, because we used $S = \infty$ in the paramagnetic region, the fit between theory and experiment only has meaning for $S = \frac{5}{2}$ ions, as is the case of Fe(III).

ACKNOWLEDGMENTS

The Comisión Asesora de Investigacion Científica y Técnica supported the contribution at Universidad de Zaragoza and the National Science Foundation (Solid State Chemistry Program of the Division of Materials Research under Grants No. DMR-79-06119 and No. DMR-82-11237) supported the contribution at University of Illinois.

[1] J. A. Puertolas, R. Navarro, F. Palacio, J. Bartolome, D. Gonzalez, and R. L. Carlin, Phys. Rev. B **26**, 395 (1982).
[2] C. J. O'Connor, B. S. Deaver, and E. Sinn, J. Chem. Phys. **70**, 5161 (1979).
[3] J. E. Greedan, D. C. Hewith, R. Faggiani, and I. D. Brown, Acta Crystallogr. Sect. B **36**, 1927 (1980).
[4] R. L. Carlin, S. N. Bhatia, and C. J. O'Connor, J. Am. Chem. Soc. **99**, 7728 (1977).
[5] B. N. Figgis, C. L. Raston, R. P. Sharma, and A. H. White, Aust. J. Chem. **31**, 2717 (1978).
[6] J. N. McElearney and S. Merchant, Inorg. Chem. **17**, 1207 (1978).
[7] J. A. Puertolas, Ph.D. thesis, Universidad de Zaragoza, 1980 (unpublished).
[8] C. J. O'Connor, Ph.D. thesis, University of Illinois at Chicago Circle, 1976 (unpublished).
[9] F. Palacio, A. Paduan-Filho, and R. L. Carlin, Phys. Rev. B **21**, 296 (1980).
[10] S. K. Misra and G. R. Sharp, J. Chem. Phys. **66**, 4172 (1977).
[11] D. N. Lambeth and H. E. Stanley, Phys. Rev. B **12**, 5302 (1975).
[12] G. S. Rushbrooke, G. A. Baker, Jr., and P. J. Wood, in *Phase Transitions and Critical Phenomena,* edited by C. Domb and M. S. Green (Academic, New York, 1974).
[13] G. S. Rushbrooke and P. J. Wood, Mol. Phys. **6**, 409 (1963).
[14] R. Navarro, Ph.D. thesis, Universidad de Zaragoza, 1976 (unpublished).
[15] J. A. Puertolas, R. Navarro, F. Palacio, J. Bartolome, D. Gonzalez and R. L. Carlin, J. Magn. Magn. Mater. **31—34**, 1243 (1983).
[16] G. A. Baker, Jr., H. E. Gilbert, J. Eve, and G. S. Rushbrooke, Phys. Rev. **164**, 800 (1967).
[17] M. Ferer, M. A. Moore, and M. Wortis, Phys. Rev. B **4**, 3954 (1971).
[18] R. G. Bowers and M. E. Woolf, Phys. Rev. **117**, 917 (1969).
[19] C. Domb and R. G. Bowers, J. Phys. C **2**, 755 (1969).
[20] T. H. K. Barrou and J. A. Morrison, Can. J. Phys. **35**, 799 (1957).
[21] F. Keffer, in *Encyclopedia of Physics,* edited by H. P. J. Wijn (Springer, Berlin, 1967), Vol. XVIII.
[22] J. Bartolome, R. Burriel, F. Palacio, D. Gonzalez, R. Navarro, J. A. Rojo, and L. J. de Jongh, Physica (Utrecht) **115B**, 190 (1983).
[23] K. Pirnie, P. J. Wood, and J. Eve, Mol. Phys. **11**, 551 (1966).
[24] R. Navarro and L. J. de Jongh, Physica (Utrecht) **94B**, 67 (1978).